European Journal of Nuclear Medicine and Molecular Imaging
https://doi.org/10.1007/s00259-024-06778-8

EDITORIAL

Can we use PET to quantify mu opioid receptors across the monkey brain, spinal cord and peripheral organs at the same time? Totally!

Peter J. H. Scott[1,2,3]

Improving the resolution and sensitivity of positron emission tomography (PET) scanners is an ongoing quest, with new gating methods, time-of-flight, iterative reconstruction, and integration of anatomical (MRI and CT) imaging, as well as development of new detectors, just some of the approaches being investigated. These efforts have been highly successful, apparent through improvements in image quality for patient studies over the years, and comparison of images from early PET scanners with the exquisite images obtained from the latest PET/CT and PET/MRI devices [1]. Nevertheless, because PET detectors have an axial coverage of 15–30 cm, only a limited number of coincidence photons are detected and, until quite recently, whole body scans needed to be acquired using multiple bed positions in series. To address this inherent limitation, the last decade has witnessed the introduction of total body PET (TBP) scanners, extended axial field of view (e.g. 194 cm) instruments with many more detectors than traditional scanners that greatly improve upon the sensitivity of traditional PET scanners by detecting most of the coincidence photons from the whole body at once (Fig. 1) [2].

Initial funding from the National Cancer Institute's "*provocative questions award*" created the EXPLORER Consortium, a group charged with developing 2 TBP systems based upon lutetium–yttrium oxyorthosilicate (LYSO) crystals. The first, developed by the University of Pennsylvania working with Phillips and KAGE Medical, was to have excellent timing resolution and a length of 140 cm (PennPET Explorer, Fig. 2) [3, 4]. The second was a 194 cm scanner with excellent spatial resolution developed by the UC Davis team and United Imaging Healthcare (Explorer TBP) [2]. Subsequently, United has also worked with investigators at Yale to design the Neuro eXplorer, a next-generation ultra-high performance scanner, also utilizing LYSO crystals, and specifically introduced for human brain PET [5], while the main scanner manufacturers have introduced their own TBP systems (e.g. Siemens Biograph Vision Quadra (105 cm FOV, lutetium oxoorthosilicate (LSO) crystals) [6], GE Omni Legend (up to 128 cm FOV, bismuth germanate (BGO) crystals)) [7].

While TBP scanners are still somewhat in their infancy, and thus still come at quite a high cost (ca. $10 m) because of the newness of the technology and the very high numbers of crystals they contain (Explorer has 564,480 crystal elements!), the clinical benefits of such scanners resulting from the long axial field of view are numerous, including:

- Higher sensitivity (up to 68 times higher than PET/CT has been suggested [8]);
- The higher number of detectors enables dynamic acquisition from all tissues of interest at the same time;
- Improved signal-to-noise ratio (SNR);
- Shorter scan times (e.g. ≤ 10 min) with less injected dose;
- Pediatric scans can be conducted without anesthesia;

These advanced capabilities offer exciting possibilities for research and development, as well as clinical care [2, 9]. Much has been reported on the clinical use of TBP, including the first human studies with the United Imaging/UC Davis Explorer, reported in 2019 [10], and acquired using [^{18}F]fludeoxyglucose ([^{18}F]FDG). This was the first study to show [^{18}F]FDG kinetics throughout the entire body, and the team showed that diagnostic-quality scans could be acquired in ≤ 1 min! Additionally, diagnostic-quality images could also be obtained using injected doses as low as 25 MBq (0.7 mCi). Lastly, Explorer has the ability to image [^{18}F]FDG distribution for up to 10 h (< 5 half-lives) after injection given its high sensitivity.

✉ Peter J. H. Scott
pjhscott@umich.edu

[1] Department of Radiology, University of Michigan, Ann Arbor, MI 48109, USA

[2] Department of Pharmacology, University of Michigan, Ann Arbor, MI 48109, USA

[3] Department of Medicinal Chemistry, University of Michigan, Ann Arbor, MI 48109, USA

Published online: 01 June 2024

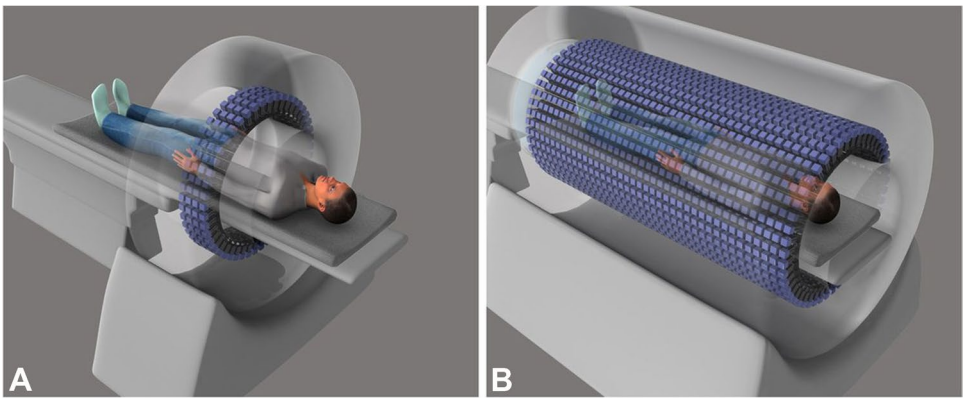

Fig. 1 Traditional PET scanner (**A**) and total-body PET (TBP) scanner (**B**). Reprinted from [2] with permission from AAAS

Fig. 2 PennPET Explorer; reproduced with permission from ref [4], © SNMMI

Meanwhile, clinical imaging with the PennPET Explorer was reported in 2020 by Pantel and colleagues. Clinical scans were acquired using [^{18}F]FDG (Fig. 3) and [^{68} Ga] DOTATATE, while research subjects were imaged with experimental radiotracers such as ^{18}F-labeled NOS PET and [^{18}F]fluortriopride [11]. Similarly, the first clinical experience with the Siemens Biograph Vision Quadra PET/CT scanner was reported in 2021 by the group from Bern, Switzerland [6, 12]. The scanners have demonstrated similar performance, providing exquisite clinical images and exciting new data far beyond the capabilities of standard scanners. Recent review articles dig deeper into the performance characteristics of the different scanners available today, as well as consider future prospects for TBP [8, 13, 14].

While much has been reported about the clinical capabilities of the long axial field of view scanners, to date comparatively less has been discussed about the enormous potential TBP scanners offer to groups engaged in pre-clinical research, both with new radiotracers and by revisiting existing tracers. In 2018, Berg and colleagues reported non-human primate imaging using mini-EXPLORER, a dedicated long axial field-of-view PET scanner for animals with a 45.7 cm axial FOV [15]. Rhesus monkeys were imaged using [^{18}F]FDG. Dynamic scans were undertaken, demonstrating similar benefits to the clinical scans noted above, including fast imaging (1-s early frames), exceptional scan quality (30-s and 5-min frames), and the ability to conduct late imaging (18 h after injection), all acquired from a single bed position capturing all the major organs of the rhesus monkeys (Fig. 4).

Now, in a recent paper in *the European Journal of Nuclear Medicine and Molecular Imaging (EJNMMI)*, Hsieh and co-workers report total-body imaging of mu-opioid receptors (MORs) with [^{11}C]carfentanil ([^{11}C]CFN) in non-human primates (NHPs) on the PennPET Explorer [16]. The team is part of the PET Addiction Center of Excellence (PACE), a Center that combines expertise in PET and opioid research from the PET Centers at the University of Pennsylvania and

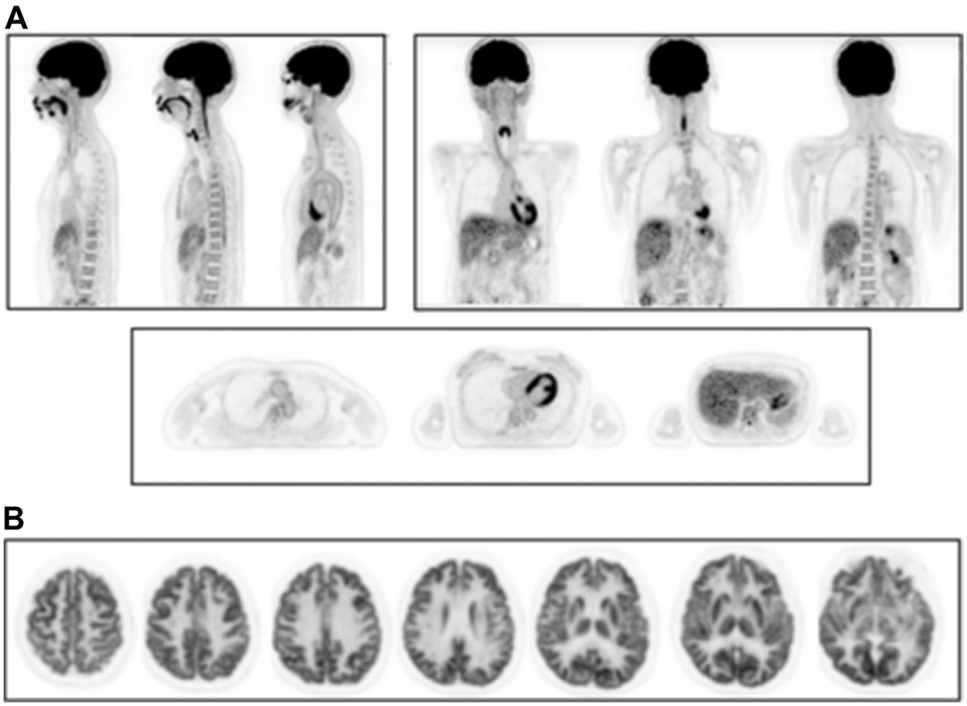

Fig. 3 **A** sagittal, coronal, and axial [^{18}F]FDG PET images of subject scanned on PennPET Explorer (10-min scan). **B** Transverse images on Penn-PET Explorer after subject was moved so that brain was positioned in center of axial FOV (10-min scan). Reproduced from [11] with permission, © SNMMI

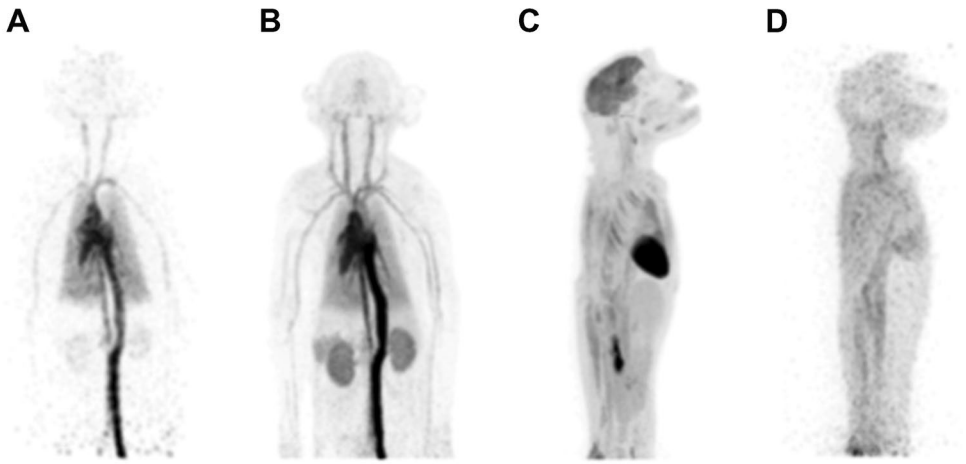

Fig. 4 Maximum-intensity-projection images from [^{18}F]FDG rhesus monkey study: 1-s frame at 5 s after injection (**A**), 0–30 s after injection (**B**), 55–60 min after injection (**C**), and 18 h after injection (40-min scan) (**D**). Reproduced from ref [15] with permission, © SNMMI

Yale University that is funded by a P30 grant through the National Institute on Drug Abuse (NIDA). The paper reports an exciting study as it represents the first work quantifying receptor occupancy in the monkey brain and the periphery at the same time using preclinical TBP. Both baseline and blocking studies were conducted to measure the effect of antagonists on MOR binding in both the CNS and peripheral organs concurrently, given the whole rhesus monkey fits in the extended axial FOV (Fig. 5).

The PennPET Explorer was used for MOR total-body PET imaging of four rhesus macaques using [^{11}C]CFN. Monkeys were scanned under baseline conditions and naloxone pretreatment (Figs. 5 and 6), as well as naloxone or GSK1521498 displacement studies. An initial low dose CT scan confirmed positioning and attenuation correction. Monkeys then received intravenous injection of 105 MBq (2.8 mCi) of [^{11}C]CFN (injected mass: 102.8 ± 207.2 ng/kg), followed by dynamic PET image acquired in list-mode. For the baseline, retest, and naloxone pretreatment scans, 90 min dynamic images were acquired in 29 time frames. For the displacement studies, naloxone or GSK1521498 was administered 40 min post-injection of [^{11}C]CFN, and the dynamic scan was continued for a total of 120 min in 48 time frames. Images were analyzed using Pmod, following co-registration to MR-T1 weighted brain images spatially normalized to the D99 rhesus macaque MR brain template. Fifteen volumes of interest (VOIs) were defined using the spatially normalized brain PET image in the D99 template domain

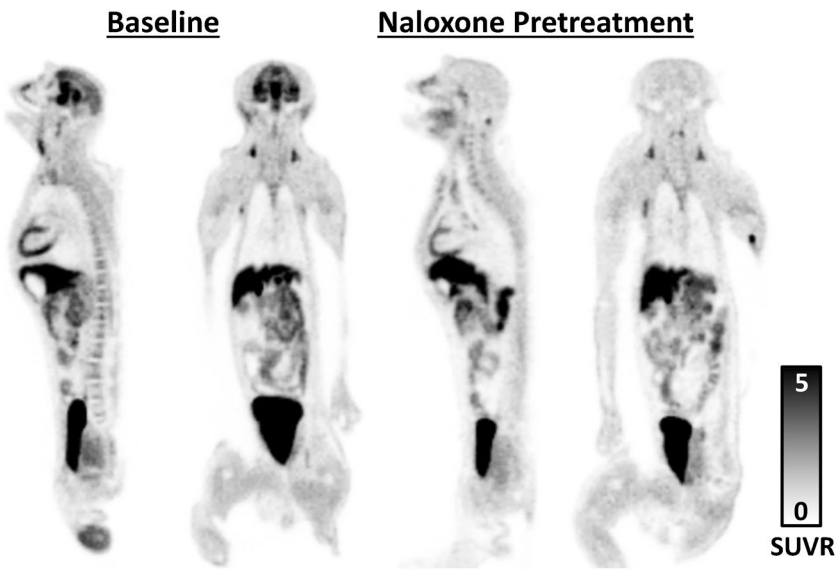

Fig. 5 Representative total-body $SUVR_{70–90\ min}$ images of the same rhesus monkey in baseline and naloxone pretreatment studies. Reproduced from ref [16] with permission

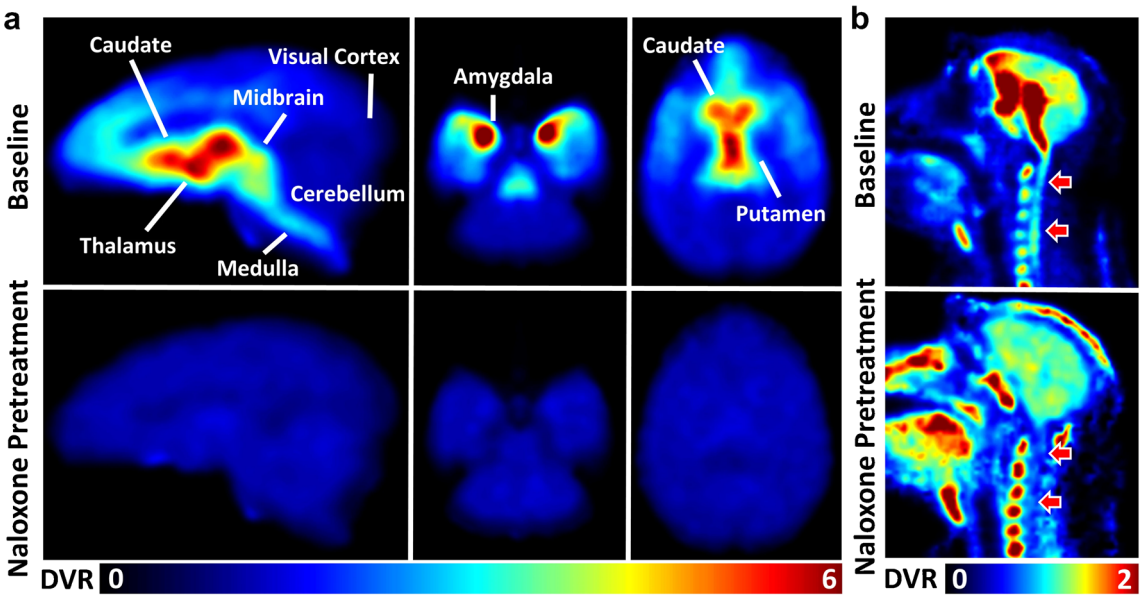

Fig. 6 Representative Logan DVR images of the same NHP in baseline and naloxone pretreatment studies in (**a**) brain and (**b**) cervical spinal cord. Reproduced from ref [16] with permission

to generate regional brain time-activity curves (TACs). The TACs of each VOI were used to calculate DVRs for control and blockade to determine the effect of the blocking agent (Logan method using cerebellar cortex as reference region). SUV ratios (SUVRs) of the various VOIs to the cerebellar cortex were also calculated.

The study demonstrates TBP and test–retest variability of [^{11}C]CFN, a MOR agonist radiotracer that has been used for opioid imaging since the 1980s. Baseline studies using the PennPET Explorer revealed high radiotracer uptake in brain regions known to express MOR (thalamus, caudate, putamen, nucleus accumbens, amygdala, hippocampus, midbrain), while test–retest variability in the brain was found to be 8%, in line with prior reports over the years. Capitalizing on the TPB capabilities of their new scanner (i.e. extended FOV and high sensitivity), the team was able to quantify [^{11}C]CFN signal in the cervical spinal cord (Fig. 6) and also found high reproducibility of the DVR (~6% test–retest variation). In the naloxone pretreatment studies, a significant blocking effect was observed in most of the brain regions as well as in cervical spinal cord (Fig. 6). In displacement studies, the ability of naloxone and GSK1521498 to prevent the [^{11}C]CFN rebinding to the MOR was found to be similar, and no differences

were observed in the rate of "displacement" of [^{11}C]CFN between the two antagonists.

Finally, the authors demonstrate clear advantages to monkey imaging using TBP over existing scanners as they were able to study [^{11}C]CFN uptake and quantify MOR expression in the periphery, concurrent with brain and spinal cord (Figs. 5 and 6). Examining [^{11}C]CFN binding throughout the monkey revealed some expected findings (e.g. there was no difference among the TACs for the baseline, retest, and naloxone pretreatment studies in the skeletal muscle, consistent with reports of low MOR expression in that tissue). The data shown in Fig. 6 indicate the feasibility of imaging MOR in the cervical spinal cord using [^{11}C]CFN, whereas it is likely not possible in the thoracic and lumber spinal cord due to low uptake of the radiotracer. There is ambiguity around expression of MORs in the heart and, indeed, the authors found the same in this work. Naloxone pretreatment, for example, resulted in an average of 17% reduction in [^{11}C]CFN $SUVR_{70-90\ min}$ for 2 monkeys, but a 4% increase in the third, and mixed results in the fourth. In the displacement studies, a gradual change in [^{11}C]CFN signal after treatment with naloxone or GSK1521498 was observed in the TACs. The authors suggest that perhaps dosing at 0.14 mg/kg may not be high enough to block the binding of [^{11}C]CFN to cardiac MORs. Presumably, there could also be variations in MOR expression between the animals (e.g. due to age, sex etc.). Either way, additional studies are warranted and the TBP capabilities of the PennPET Explorer will be critical to answering such questions. Lastly, of note, somewhat higher test–retest variability was apparent in some peripheral organs compared with the brain and cervical spinal cord, which the authors attribute to complications in quantification due to the expected presence of labeled metabolites outside of the brain and/or variability of the biological clearance of [^{11}C]CFN and its radiolabeled metabolites amongst the NHPs.

This new generation of TBP scanners are already having a pronounced impact on clinical brain PET, enabling identification, and thus quantification, of very small brain regions beyond the resolution of more traditional PET scanners [17]. Prior work from Berg [15], and the new study in *EJNMMI* from Hsieh and colleagues [16], show that there is also much to be learned from TBP in the preclinical setting. Overall, the paper describing the first animal imaging study using the PennPET Explorer represents a milestone in the development of TBP. In this case, the use of total body PET in combination with both blocking and displacement studies enabled study of the dynamic interactions between the MOR agonist [^{11}C]CFN and MOR antagonists like naloxone and GSK1521498 across the brain, spinal cord and peripheral organs simultaneously. The findings are important in the context of opioid PET, and are certain to be useful as we wrangle with the opioid crisis and ongoing efforts to develop non-addictive opioid painkillers.

Furthermore, in addition to obtaining exquisite brain images and showing high test-test repeatability, this proof-of-concept study demonstrated that preclinical TBP enables evaluation of receptor expression and target engagement in the brain and across the entire monkey in a single scan. From an academic perspective, one can see how this capability will rapidly lead to a trove of imaging data that ordinarily might be missed. Traditional monkey scanners do not have adjustable beds and/or animals cannot be kept under anesthesia for extended periods of time to scan in multiple bed positions while, other times, there is insufficient scanner bandwidth and/or research funds to acquire multiple scans for every new tracer/drug under evaluation. Thus, the ability to acquire extensive imaging data from both the brain and periphery during a single scan represents a gamechanger for preclinical PET. The new insights into whole body pharmacokinetics and target engagement that TBP is enabling are expected to improve the process of tracer development (e.g. use of lower doses is beneficial when early phase radiosyntheses might still be low yielding [18, 19], TBP image-derived input functions could reduce/eliminate the need for arterial blood sampling [20]) as well as further enhance the use of PET imaging in drug development, allowing drug hunters to gain significantly more information about their pharmaceutical assets (e.g. target expression/ engagement, off target interactions, drug sinks etc.) without added experimental complexity or need for additional scans. Today, TBP scanners remain costly, but given that the price is expected to drop and the benefits continue to become apparent, TBP technology is expected to become more commonplace in the future presenting exciting new possibilities for translational imaging scientists working in nuclear medicine and theranostics.

Data availability Complete data used to support the findings of the study can be found in the original article.

Declarations

Ethics approval Institutional Review Board approval was not required because the paper is an Editorial.

Consent to participate Not applicable.

Conflict of interest The author declares no competing interests.

References

1. Jones T, Townsend D. History and future technical innovation in positron emission tomography. J Med Imaging (Bellingham). 2017;4(1): 011013.
2. Cherry SR, Badawi RD, Karp JS, Moses WW, Price P, Jones T. Total-body imaging: transforming the role of positron emission tomography. Sci Transl Med. 2017;9:eaaf6169.

3. Karp J, Schmall J, Geagan M, Werner ME, Parma MJ, Matej S, Daube-Witherspoon ME, Viswanath V, McDermott T, Muehlleher G, Perkins A, Tung C-H. Imaging performance of the PennPET Explorer scanner. J Nucl Med. 2018;59(suppl 1):222.
4. Karp JS, Viswanath V, Geagan MJ, Muehllehner G, Pantel AR, Parma MJ, Perkins AE, Schmall JP, Werner ME, Daube-Witherspoon ME. PennPET Explorer: design and preliminary performance of a whole-body imager. J Nucl Med. 2020;61(1):136–43.
5. Carson R, Berg E, Badawi R, Cherry S, Du J, Feng T, Fontaine K, Gravel P, Hillmer A, Honhar P, Hoye J, Hu L, Jones T, Leung E, Li T, Liu C, Liu H, Lu Y, Majewski S, Mulnix T, Schmall J, Selfridge A, Toyonaga T, Qi J, Li H. Design of the NeuroEXPLORER, a next-generation ultra-high performance human brain PET imager. J Nucl Med. 2021;62(1):1120.
6. Prenosil GA, Sari H, Fürstner M, Afshar-Oromieh A, Shi K, Rominger A, Hentschel M. Performance characteristics of the biograph vision quadra PET/CT system with a long axial field of view using the NEMA NU 2–2018 standard. J Nucl Med. 2022;63:476–84.
7. Yamagishi S, Miwa K, Kamitaki S, Anraku K, Sato S, Yamao T, Kubo H, Miyaji N, Oguchi K. Performance characteristics of a new-generation digital bismuth germanium oxide PET/CT system, omni legend 32, according to NEMA NU 2–2018 standards. J Nucl Med. 2023;64:1990–7.
8. Katal S, Eibschutz LS, Saboury B, Gholamrezanezhad A, Alavi A. Advantages and applications of total-body PET scanning. Diagnostics (Basel). 2022;12:426.
9. Cherry SR, Jones T, Karp JS, Qi J, Moses WW, Badawi RD. Total-Body PET: maximizing sensitivity to create new opportunities for clinical research and patient care. J Nucl Med. 2018;59:3–12.
10. Badawi RD, Shi H, Hu P, Chen S, Xu T, Price PM, Ding Y, Spencer BA, Nardo L, Liu W, Bao J, Jones T, Li H, Cherry SR. First human imaging studies with the EXPLORER total-body PET scanner. J Nucl Med. 2019;60:299–303.
11. Pantel AR, Viswanath V, Daube-Witherspoon ME, Dubroff JG, Muehllehner G, Parma MJ, Pryma DA, Schubert EK, Mankoff DA, Karp JS. PennPET Explorer: human imaging on a whole-body imager. J Nucl Med. 2020;61:144–51.
12. Alberts I, Hünermund JN, Prenosil G, Mingels C, Bohn KP, Viscione M, Sari H, Vollnberg B, Shi K, Afshar-Oromieh A, Rominger A. Clinical performance of long axial field of view PET/CT: a head-to-head intra-individual comparison of the Biograph Vision Quadra with the Biograph Vision PET/CT. Eur J Nucl Med Mol Imaging. 2021;48:2395–404.
13. Roya M, Mostafapour S, Mohr P, Providência L, Li Z, van Snick JH, Brouwers AH, Noordzij W, Willemsen ATM, Dierckx RAJO, Lammertsma AA, Glaudemans AWJM, Tsoumpas C, Slart RHJA, van Sluis J. Current and future use of long axial field-of-view positron emission tomography/computed tomography scanners in clinical oncology. Cancers (Basel). 2023;15:5173.
14. Alberts I, Sari H, Mingels C, Afshar-Oromieh A, Pyka T, Shi K, Rominger A. Long-axial field-of-view PET/CT: perspectives and review of a revolutionary development in nuclear medicine based on clinical experience in over 7000 patients. Cancer Imaging. 2023;23:28.
15. Berg E, Zhang X, Bec J, Judenhofer MS, Patel B, Peng Q, Kapusta M, Schmand M, Casey ME, Tarantal AF, Qi J, Badawi RD, Cherry SR. Development and evaluation of mini-EXPLORER: a long axial field-of-view PET scanner for nonhuman primate imaging. J Nucl Med. 2018;59:993–8.
16. Hsieh CJ, Hou C, Lee H, et al. Total-body imaging of mu-opioid receptors with [^{11}C]carfentanil in non-human primates. Eur J Nucl Med Mol Imaging. 2024. https://doi.org/10.1007/s00259-024-06746-2.
17. Carson R, Toyonaga T, Badawi R, Cherry S, Du J, Fontaine K, Gallezot J-D, Gravel P, He L, Hillmer A, Holderman N, Honhar P, Jocelyn H, Hu L, Jones T, Khattar N, Leung E, Li T, Li Y, Liu C, Liu P, Lu Z, Majewski S, Matuskey D, Morris E, Mulnix T, Raval N, Samanta S, Selfridge A, Shanina E, Sun X, Volpi T, Xie Z, Xu T, Zeng T, Zhang J, Zhang X, Franco A, Masdeu J, Fujita M, Qi J, Li H. Exceptional PET Images from the First Human Scan on the NeuroEXPLORER, a next-generation ultra-high performance brain PET imager. J Nucl Med. 2023;64(Suppl. 1):P298.
18. de Vries EFJ, Elsinga PH, Tsoumpas C. Will extended field-of-view PET/CT depopulate the graveyard of failed PET radiopharmaceuticals? Cancer Imaging. 2022;22:70.
19. Kiss OC, Scott PJH, Behe M, Penuelas I, Passchier J, Rey A, Patt M, Aime S, Jalilian A, Laverman P, Cheng Z, Chauvet AF, Engle J, Cleeren F, Zhu H, Vercouillie J, van Dam M, Zhang MR, Perk L, Guillet B, Alves F. Highlight selection of radiochemistry and radiopharmacy developments by editorial board. EJNMMI Radiopharm Chem. 2023;8:6.
20. Zhu Y, Tran Q, Wang Y, Badawi RD, Cherry SR, Qi J, Abbaszadeh S, Wang G. Optimization-derived blood input function using a kernel method and its evaluation with total-body PET for brain parametric imaging. Neuroimage. 2024;293: 120611.